Chemico-Biological Interactions 220 (2014) 200–207

Contents lists available at ScienceDirect

Chemico-Biological Interactions

journal homepage: www.elsevier.com/locate/chembioint

DNA-binding studies of AV-153, an antimutagenic and DNA repair-stimulating derivative of 1,4-dihydropiridine

E. Buraka [a,b], C. Yu-Chian Chen [c,d], M. Gavare [e], M. Grube [e], G. Makarenkova [f], V. Nikolajeva [f], I. Bisenieks [b], I. Brūvere [b], E. Bisenieks [b], G. Duburs [b], N. Sjakste [a,b,*]

[a] Department of Medical Biochemistry, Faculty of Medicine, University of Latvia, No. 4 Kronvalda Boulevard, Riga LV-1010, Latvia
[b] Latvian Institute of Organic Synthesis, No. 21 Aizkraukles Street, Riga LV-1006, Latvia
[c] Laboratory of Computational and Systems Biology, School of Chinese Medicine, China Medical University, Taichung 40402, Taiwan
[d] Department of Bioinformatics, Asia University, Taichung 41354, Taiwan
[e] Institute of Microbiology and Biotechnology, University of Latvia, No. 4 Kronvalda Boulevard, Riga LV-1010, Latvia
[f] Faculty of Biology, University of Latvia, No. 4 Kronvalda Boulevard, Riga LV-1010, Latvia

ARTICLE INFO

Article history:
Received 27 December 2013
Received in revised form 20 June 2014
Accepted 30 June 2014
Available online 10 July 2014

Keywords:
1,4-Dihydropyridines
DNA intercalation
Antimutagenic compounds
UV/VIS spectroscopy
Fluorimetry
FTIR

ABSTRACT

The ability to intercalate between DNA strands determines the cytotoxic activity of numerous anticancer drugs. Strikingly, intercalating activity was also reported for some compounds considered to be antimutagenic. The aim of this study was to determine the mode of interaction of DNA with the antimutagenic and DNA repair-stimulating dihydropyridine (DHP) AV-153. DNA and AV-153 interactions were studied by means of UV/VIS spectroscopy, fluorimetry and infrared spectroscopy.

Compound AV-153 is a 1,4 dihydropyridine with ethoxycarbonyl groups in positions 3 and 5. Computer modeling of AV-153 and DNA interactions suggested an ability of the compound to dock between DNA strands at a single strand break site in the vicinity of two pyrimidines, which was confirmed in the present study. AV-153 evidently interacted with DNA, as addition of DNA to AV-153 solutions resulted in pronounced hyperchromic and bathochromic effects on the spectra. Base modification in a plasmid by peroxynitrite only minimally changed binding affinity of the compound; however, induction of single-strand breaks using Fenton's reaction greatly increased binding affinity. The affinity did not change when the ionic strength of the solution was changed from 5 to 150 mM NaCl, although it increased somewhat at 300 mM. Neither was it influenced by temperature changes from 25 to 40 °C, however, it decreased when the pH of the solution was changed from 7.4 to 4.7. AV-153 competed with EBr for intercalation sites in DNA: 116 mM of the compound caused a two-fold decrease in fluorescence intensity. FT-IR spectral data analyses indicated formation of complexes between DNA and AV-153. The second derivative spectra analyses indicated interaction of AV-153 with guanine, cytosine and thymine bases, but no interaction with adenine was detected.

Conclusions: The antimutagenic substance AV-153 appears to intercalate between the DNA strands at the site of a DNA nick in the vicinity of two pyrimidines.

1. Introduction

DNA damage by irradiation, chemicals, endogenous free radicals, and further ineffective repair of these lesions are common causes of premature aging, cancer [1,2] and other diseases including *diabetes mellitus* [3,4] and neuropathies [5]. Treatment strategies of cancer and *diabetes mellitus* can be aimed at DNA damage prevention and DNA repair enhancement [6,7].

The necessity to protect DNA against damage stimulates great interest in natural and synthetic compounds with antioxidant and antimutagenic properties [8].

Antimutagens are defined as agents, which decrease the mutagenicity of a substance either by preventing its transformation into a mutagen, or by inactivation, or by preventing a mutagen–DNA reaction. Some of them are reported to interact directly with DNA. Morin, quercetin, ellagic acid, genistein, baicalein and rutin bind effectively to DNA through intercalation. Although this effect is characteristic of mutagens, most of these compounds are considered to be antimutagenic [9–15]. Quercetin, kaempferol and delphinidin can also intercalate in DNA [16]. Some researchers insist

* Corresponding author at: Department of Medical Biochemistry, Faculty of Medicine, University of Latvia, No. 4 Kronvalda Boulevard, Riga LV-1010, Latvia.
E-mail address: nikolajs2000@yahoo.com (N. Sjakste).

http://dx.doi.org/10.1016/j.cbi.2014.06.027
0009-2797/

that DNA-binding activity of the above compounds cannot result in mutagenesis [11,12]. Thus, direct binding of antimutagens to DNA could be a possible mechanism of their DNA-protecting action.

Synthetic derivatives of 1,4-dihydropyridine (1,4-DHPs) possess important biochemical and pharmacological properties. Some β-carbonyl-1,4-dihydropyridine analogues of dihydronicotinamide, the hydrogen- and electron-transferring moiety of the redox coenzymes NADH and NADPH, manifest antimutagenic activity. 1,4-DHPs apparently inhibit chemical mutagenesis due to modulation of DNA repair. Study of the impact of DHP on DNA repair indicated that the DHP derivative AV-153 reduced the number of DNA strand breaks not only in untreated cells, but also in cells exposed to gamma-radiation, ethylmethane sulfonate, or H_2O_2 [17,18]. The similarity of 1,4 DHP and nicotinamide chemical structures suggests that AV-153 stimulates DNA repair by increasing poly(ADP ribose) synthesis. Indeed, the level of poly(ADP ribose) after genotoxic stress increases more than twofold in presence of AV-153 [19].

The aim of this study was to determine the mode of interaction of DNA with the antimutagenic and DNA repair stimulating dihydropyridine (DHP), AV-153.

2. Materials and methods

2.1. Chemicals

AV-153 sodium salt was synthesized in the Laboratory of Membrane Active Compounds at the Latvian Institute of Organic Synthesis. The structure of the compound is given in Fig. 1A. Tris base, sucrose, Triton-X-100, Hind III/λ DNA digest, ethidium bromide (EBr), hydroxyapatite, Na_2EDTA, LiCl, NaCl, $CaCl_2$ and other inorganic salts were purchased from Sigma–Aldrich. 2-mercaptoethanol was obtained from Ferak Berlin, sodium dodecyl sulfate was supplied by Acros Organics, isoamylic alcohol was obtained from Stanlab, and 6× Orange loading solution, RNase A and Proteinase K were purchased from Fermentas.

2.2. Oligonucleotides

Oligonucleotides were supplied by Metabion. The single-stranded oligonucleotide SNP20222-F 5′-ACC AGG CAA CAT CTT GAA GG-3′ was designed by T. Sjakste. Sequences of published palindromic hairpin-forming oligonucleotides were as follows:

1) "*AT Rich*" 5′-AAG AAT TCT TAA GAA TTC TT-3' [20].
2) "*CG-Center*"-5′-GGT ACC GGT ACC-3′ [21].
3) "*ALS2*"-5′-GCG CAT GCG CGC GCA TGC GC-3′ [22].

2.3. Isolation of DNA from rat liver

DNA was isolated from the liver of Wistar rats, as rat liver is a convenient source for easy purification of DNA in large quantities. Chopped liver tissue was placed in a Dounce homogenizer, and a 10-fold excess of homogenization buffer (w/v) consisting of 0.25 M sucrose, 0,05 M Tris–HCl at pH 7.4 and 0,002 M $CaCl_2$ was added. After ten strokes, homogenate was centrifuged at 1000 *g* for 10 min. The pellet was again homogenized in a buffer containing 50 mM Tris–HCl at pH 7.5, 0.25 M sucrose, 2 mM $CaCl_2$, and 1% Triton X-100. Crude nuclei were pelleted at 1000*g* for 10 min. Extraction was repeated. The nuclear pellet was mixed with an appropriate amount of buffer (100 mM Tris–HCl at pH 7.5, 500 mM NaCl, 50 mM Na_2EDTA, 1.25% $NaDodSO_4$, 3.8 g/l of sodium bisulfite, and 4 ml/l of 2-mercaptoethanol). The two latter components were added to the buffer just before extraction to obtain a slightly viscous suspension. The lysate was incubated for 45 min at 65 °C. DNA was extracted with the same volume of chloroform/isoamylic alcohol mixture (24:1), the suspension was centrifuged, and the water phase was separated. RNA was separated by precipitation in 4 M LiCl at 4 °C for at least one hour, and a 12 M LiCl solution was added to the water phase to reach the necessary salt concentration. RNA was pelleted for 10 min at 10,000*g*. The chloroform extraction procedure of the supernatant was repeated again. DNA was precipitated from the water phase with two volumes of ethanol and washed in 70% ethanol. The DNA pellet was dried and diluted in water. To purify the DNA sample of possible protein and RNA contaminants, it was first treated with RNase A (50 mg/ml, 1 h, 65 °C), then Proteinase K (400 mg/ml) and 1.25% $NaDodSO_4$ (1 h, 65 °C). The mixture was extracted with chloroform/isoamyl alcohol; DNA was precipitated, dried and dissolved in water up to 7.48 mM.

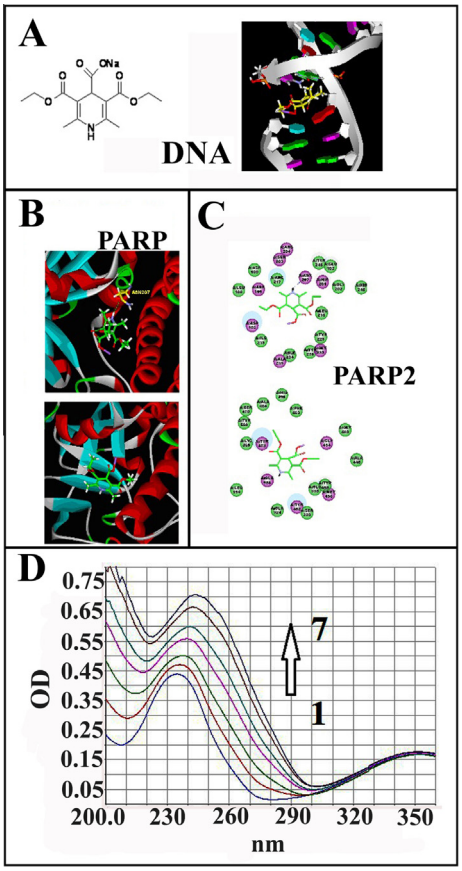

Fig. 1. (A) Chemical structure of AV-153. (B) Model of interaction with DNA. (C) Docking position and 2D diagram of AV-153 in binding sites of PAPR-1 and PARP2. The green and purple colors denote residues with polar and van der Waals interaction, respectively. (D) UV–VIS spectra of AV-153 sodium salt in the absence and presence of different concentrations of rat liver DNA: blue – 0 μM DNA, red – 6,5 μM, green 13 μM, magenta – 19,5 μM, cyan – 26 μM, brown – 32,5 μM, black – 39 μM.

2.4. Isolation of genomic DNA from bacteria

Cultures of *Staphylococcus aureus* MSCL 334 and *Micrococcus luteus* MSCL 25 were obtained from the Microbial Strain Collection of Latvia. *S. aureus* was cultivated in nutrient broth (Difco) at 37 °C for 48 h. *M. luteus* was cultivated on plate count agar (Oxoid) at 22 °C for 72 h and bacterial biomass was collected and suspended in sterile water. Bacteria were spun down and suspended in TE buffer with lysozyme (10 mM Tris–HCl at pH 8.0, 1 mM EDTA; 20 mg/ml lysozyme, 1% Triton X-100) and incubated at room temperature for 20 min. $NaDodSO_4$ and Proteinase K were then added

up to concentrations of 1% and 100 μg/ml respectively. The mixture was kept at 55 °C for an hour. Nucleic acids were extracted with a mixture of chloroform and isoamyl alcohol (24:1). The water phase was collected, NaCl was added up to 0.1 M, and nucleic acids were precipitated with two volumes of ethanol. The pellet was dissolved in TE, and to remove bulk RNA and other contaminants, LiCl was added to 4 M, incubated on ice for an hour and centrifuged at 14,000*g* for 30 min. Nucleic acids were again precipitated with ethanol, dissolved in TE and treated first with RNase (25 μg/ml, 1 h, 37 °C), then with 1% $NaDodSO_4$ and Proteinase K (100 μg/ml) for 3 h at 50 °C. DNA was again extracted with chloroform and isoamyl alcohol and precipitated with ethanol.

2.5. Plasmid isolation

Escherichia coli DH5alpha strain was transformed with plasmid pTZ57R, the bacteria were grown in a liquid medium, and plasmid DNA was isolated according the conventional alkaline extraction protocol.

2.6. DNA sonication, purification, and dialysis

DNA samples were sonicated in a sonicator UZDN-2T (USSR) by applying five to fifteen consecutive cycles of 15 s of sonication followed by a 45 s pause. The sonicator tip was introduced directly into the solution, which was kept in an ice bath to minimize thermal effects. Agarose gel electrophoresis tests confirmed that the polymer length was reduced to fragments ranging from 2 to 0.5 Kb in length. To remove remnants of polysaccharides, DNA was fixed on hydroxyapatite in 0.12 M phosphate buffer pH 7.4 and then released from hydroxyapatite with 0.4 M phosphate buffer. The DNA was dialysed in a D-Tube Mini Dialyser (Calbiochem) against deionized water for 12 h. Spectrophotometric analysis indicated that A260/A280 ratio in the DNA samples was 1.9–2.0.

2.7. Treatment with peroxynitrite

Peroxynitrite was synthesized as described [23]. pTZ57R DNA was treated with 1 mM peroxynitrite in 0.1 M NaOH for 1 h at 37 °C. Induction of single-strand breaks was monitored by electrophoresis in alkaline conditions.

2.8. Fenton reaction

Plasmid pTZ57R DNA was treated with 0.003% H_2O_2 and 0.1 mM $FeSO_4$ for 30 min at 37 °C. The damaged DNA was dialysed against water for 24 h. The degree of DNA strand breakage was evaluated by alkaline agarose gel electrophoresis.

2.9. UV/VIS spectroscopic measurements

UV–VIS spectra were recorded with a Perkin Elmer Lambda 25 UV/VIS spectrophotometer in the absence of DNA and in the presence of increasing amounts of DNA in 5 mM NaCl and 5 mM Tris–HCl at pH 7.4 or other buffer. A 30-μM solution of the tested compound was diluted out of a 1 mM stock solution in the buffer in a quartz cell (2 ml). A reference cell was filled with 1 ml of the buffer. The mixture was mixed thoroughly and titrated by 1.2 mM DNA solution, 10 μM each time to both sample and reference cells. DNA molar concentration was calculated on the basis of absorbance of the solution at 260 nm and molar extinction coefficient for DNA. Spectra were recorded in a 400–200 nm interval at room temperature. Temperature in the thermostated cell was changed in some experiments.

Binding constants were calculated by applying the formula

$$\frac{1}{A_0 - A} = \frac{1}{A_0} + \frac{1}{K \times A_0 \times c_{DNA}}$$

according to [15], where A_0 is absorption of the free substance, A is absorption in presence of DNA, and c_{DNA} is DNA concentration.

2.10. Fluorescence spectroscopic measurements

Spectrofluorimetric analyses were performed on a Fluoromax-3 (Horiba JOBIN YVON). Fluorescence spectra of a 25-μM solution of AV-153 in 5 mM Tris–HCl; 5 mM NaCl at pH 7.4 were recorded over a range of 240–700 nm at an excitation wavelength of 350 nm. DNA was sequentially added up to 10, 50 and 100 μM. Fluorescence spectroscopic experiments on the interaction of AV-153 with the DNA-EBr complex were carried out at room temperature in 5 mM Tris–HCl; 5 mM NaCl at pH 7.4 using a 1-cm cuvette. The complex of rat liver DNA (74.8 μM) and ethidium bromide (1.26 μM) was titrated with 8.3 μM aliquots of the 2.5-mM solution of the compound. After each titration, the solution was mixed thoroughly and allowed to equilibrate for 5 min prior to fluorescence measurement. Excitation wavelength was 335 nm, and fluorescence was measured at 480 nm.

2.11. Fourier transform infrared (FT-IR) spectroscopy

Suspension of 5–10 μL of plasmid DNA, AV-153 or mixture of AV-153 and plasmid DNA in a ratio of 1:2 or 1:5, or, alternatively "oligo-GC centre" oligonucleotide solutions, were dried at $T < 50$ °C on a 384 well silicone plate. FT-IR absorption spectra were recorded on a VERTEX 70 coupled with an HTS-XT microplate reader extension (BRUKER, Germany) over a range of 4000–600 cm^{-1} with a resolution of 4 cm^{-1}, 64 scans. Baseline was corrected using the rubber band method, and CO_2 bands were excluded. For data analyses, spectra were used which fit the absorption limits of 0.25–0.80 (to fulfill the Lambert–Bouguer–Beer law where the concentration of a component is proportional to the intensity of the absorption band). Data were processed using OPUS 6.5 software.

2.12. Docking experiments

The crystal structure of DNA was obtained from Protein Data Bank (PDB: 1BNA) [24]. 2D and 3D scaffolds of test compounds were built using ChemBioOffice 2010 software. The LibDock program [25] was utilized to perform DNA-ligand interaction under Accelrys Discovery Studio 2.5.5.9350. A sphere of radius 25 Å was used to define a binding area, and polar and non-polar hotspots were regarded as active sites. The number of hotspots was set at 100 for conformer matching. The fast mode of conformation method was used to generate conformations. The final predicted DNA-ligand complex was optimized by energy minimization, with HARvard Macromolecular Mechanics (CHARMm) used as the force field for energy minimization [26], and the complex was then minimized by the conjugate gradient method. All predicted docking positions had a LibDock Score calculated for binding affinity analysis.

3. Results

3.1. Docking experiments

Docking experiments were first performed to test the hypothesized possibilities of AV-153 interacting with DNA and poly(ADP)ribose polymerases. These experiments demonstrated that intercalation can occur exclusively at sites of DNA nicks (Fig. 1A). These results were in some contradiction to previously published

data on stimulation of poly(ADP)ribose synthesis by AV-153 [18,19]. It was hypothesized that the compound could stimulate activity of the enzyme due to its structural similarity to nicotinic acid. Docking experiments also revealed the possibility of AV-153 binding to active centers of poly(ADP)ribose polymerase 1 (PARP1) and 2 (PARP2). The binding site of PARP1 was based on the location of the PARP1 inhibitor (FR257517) in the crystal structure (1UK0), and the PARP2 inhibitor 3-aminobenzamide in human PARP2 (3KCZ) was used as the binding site for docking analysis. From the docking results of AV-153 successfully bound to the inhibitory sites of PARP1 and PARP2, the binding positions and the docking score could be computed. Asn207 of PARP1 forms one H-bond with the N–H moiety of AV-153 (Fig. 1B). However, no H-bonds were observed in PARP2 (Fig. 1C), as the number of polar residues in PARP2 is less than PARP1. The docking score for PARP1 was 53.182, and for PARP2 it was 45.346. Thus, one could propose an alternative mechanism for AV-153, probably binding to DNA in the vicinity of DNA nicks. Further experiments were aimed at testing this hypothesis.

3.2. Absorption studies

Absorption titration was carried out to monitor the interaction of the compound with sonicated rat liver DNA. The UV–VIS spectra of AV-153 sodium salt in the absence and presence of different concentrations of DNA are shown in Fig. 1D. The substance has two absorption maxima at 351 and 234 nm. When the DNA solution was gradually added to the solution of AV-153, a hyperchromic effect was observed. The short-wave absorption maximum shifted to 243 nm, indicating a bathochromic effect. Thus, direct interactions between DNA and AV-153 are evident. Similar effects were observed when intact pTZ57R plasmid (Fig. 2A) or sonicated plasmid DNA (Fig. 2B) was used for titration. After induction of single-strand breaks in the plasmid DNA using the Fenton reaction, the binding affinity of the compound increased from 3.8×10^4 to 11.7×10^4 L mol^{-1} (Fig. 2C). Base modification by peroxynitrite with creation of alkali-labile sites did not significantly change the binding constant (Fig. 2D and Table 1). The binding affinity did not appreciably change when ionic strength of the solution was changed from 5 to 10, 20, 50 or 150 mM of NaCl. However, it did increase when the ionic strength of the solution was raised to 300 mM. Changes in the temperature (25, 30, 37 or 40 °C) did not influence the binding affinity. A shift in pH from 7.4 to 4.7 considerably decreased the binding affinity of AV-153 to both plasmid and rat liver DNA (Table 1).

3.3. Absorption studies of AV-153 interaction with nucleic acid fragments of different structure and composition

The compound interacted with the single-stranded oligonucleotide (Fig. 3A) and hairpin-forming oligonucleotides (Fig. 3B–D). Hyperchromic and hypochromic effects were observed. However the effects were less pronounced compared to double-stranded DNA.

Interaction of the compound with AT-rich DNA of *S. aureus* (31–37% of GC pairs [27] was comparable to interactions with GC-rich *M. luteus* DNA (about 75% of GC pairs), although it was weaker than with rat DNA (42–44% of GC pairs).

AV-153 apparently prefers interaction with DNA where GC and AT pairs are present in equal amounts.

3.4. Fluorescence measurements

The ability of AV-153 to interact with DNA was confirmed in fluorescence measurements (Fig. 4). At an excitation wavelength of 350 nm, the compound emitted light at a maximum close to maximum of the excitation light (480 nm). The intensity of fluorescence increased drastically when DNA was added to the solution. These results again confirm the direct interaction between the compound and DNA.

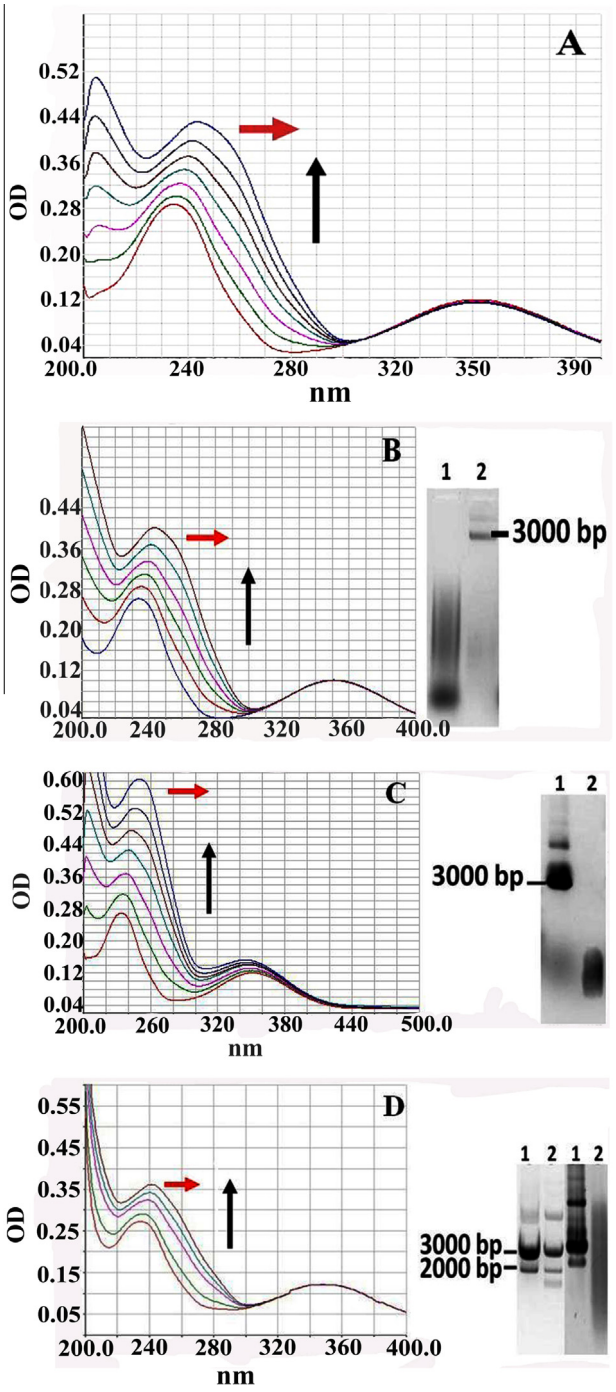

Fig. 2. AV-153-Na absorption spectra in absence and presence of plasmid pTZ57R DNA after different treatments. (A) Intact plasmid; (B) sonicated pTZ57R plasmid DNA. Insertion: gel electrophoresis at neutral conditions of sonicated (lane 1) and intact (lane 2) pTZ57R plasmid DNA. Arrows indicate positions of molecular weight markers. (C) Interactions of pTZ57R plasmid DNA treated in Fenton's reaction. Insertion: gel electrophoresis in alkaline conditions of intact (lane 1) and treated (lane 2) pTZ57R plasmid DNA. (D) pTZ57R plasmid DNA treated with peroxynitrite. Insertion: gel electrophoresis at neutral conditions (left) and alkaline conditions (right). Lane 1 – intact plasmid; lane 2 – peroxynitrite-treated plasmid.

Table 1
Binding constants of different DNA samples and AV-153.

No.	DNA sample	Conditions	Binding constant ($L\ mol^{-1}$)
1	Sonicated rat liver DNA	5 mM NaCl;5 mM Tris–HCl, pH 7.4; room temperature	3.94716×10^4
2	Intact pTZ57R plasmid	5 mM NaCl;5 mM Tris–HCl, pH 7.4; room temperature	3.8053×10^4
3	Sonicated pTZ57R plasmid	5 mM NaCl;5 mM Tris–HCl, pH 7.4; room temperature	3.33333×10^4
4	Sonicated pTZ57R plasmid	5 mM Tris–HCl pH 7.4, 10 mM NaCl, room temperature	2.47619×10^4
5	Sonicated pTZ57R plasmid	5 mM Tris–HCl pH 7.4, 20 mM NaCl, room temperature	4.00000×10^4
6	Sonicated pTZ57R plasmid	5 mM Tris–HCl pH 7.4, 50 mM NaCl, room temperature	2.637363×10^4
7	Sonicated pTZ57R plasmid	5 mM Tris–HCl pH 7.4, 150 mM NaCl, room temperature	1.848739×10^4
8	Sonicated pTZ57R plasmid	5 mM Tris–HCl pH 7.4, 300 mM NaCl, room temperature	6.087437×10^4
9	Sonicated pTZ57R plasmid	5 mM Tris–HCl pH 4.7, 5 mM NaCl, room temperature	1.142857×10^3
10	Sonicated rat liver DNA	5 mM Tris–HCl pH 4.7, 5 mM NaCl, room temperature	2.380952×10^3
10	Sonicated pTZ57R plasmid	5 mM Tris–HCl pH 7.4, 5 mM NaCl; 25 °C	2.653061×10^4
11	Sonicated pTZ57R plasmid	5 mM Tris–HCl pH 7.4, 5 mM NaCl; 30 °C	1.680672×10^4
12	Sonicated pTZ57R plasmid	5 mM Tris–HCl pH 7.4, 5 mM NaCl; 37 °C	2.44898×10^4
13	Sonicated pTZ57R plasmid	5 mM Tris–HCl pH 7.4, 5 mM NaCl; 40 °C	2.142857×10^4
14	pTZ57R plasmid treated with peroxynitrite	5 mM NaCl;5 mM Tris–HCl, pH 7.4; room temperature	2.095238×10^4
15	pTZ57R plasmid treated in Fenton's reaction	5 mM NaCl;5 mM Tris–HCl, pH 7.4; room temperature	11.71278×10^4
16	Sonicated DNA of *Staphylococcus aureus*	5 mM NaCl;5 mM Tris–HCl, pH 7.4; room temperature	3.896104×10^3
17	Sonicated DNA of *Micrococcus luteus*	5 mM NaCl;5 mM Tris–HCl, pH 7.4; room temperature	5.194805×10^3

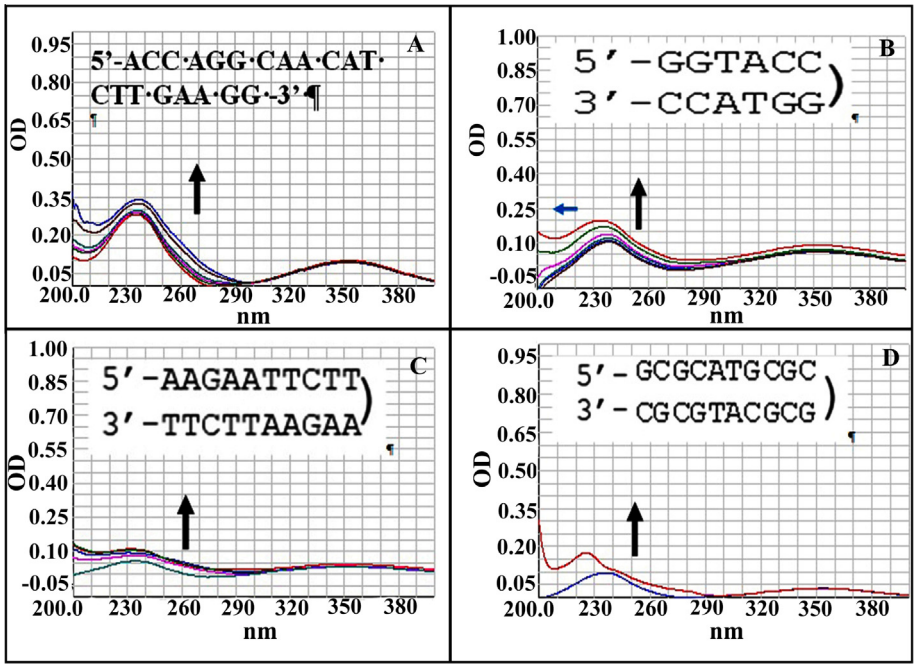

Fig. 3. AV-153 absorption spectra in absence and presence of: (A) single-strand oligonucleotide SNP20222-F; and hairpin-forming oligonucleotides (B) "CG-center", (C) "AT-rich", and (D) "ALS2". Sequences of oligonucleotides are given.

3.5. Fluorescent intercalator displacement assay

To assess the mode of DNA interactions with AV-153 we performed a fluorescence intercalator displacement assay. In this assay, the enhanced fluorescence of the DNA-EBr complex is quenched by the addition of a second ligand, which is either an intercalator or a groove binder [28]. As presented in Fig. 5, the substance quenched the EBr interaction sites in DNA. AV-153 competed with EBr for intercalation sites in DNA: 116 mM of the compound caused a twofold decrease of the fluorescence intensity, indicating ability of the substance to intercalate between the DNA strands.

3.6. Infrared spectroscopy

The FT-IR spectra of sonicated and native plasmid DNA (Fig. 6) in the region between 1700 and 1400 cm^{-1} showed absorption bands assigned to guanine (6197 cm^{-1}), thymine (1655 cm^{-1}), adenine (1608 cm^{-1}) and cytosine (1490 cm^{-1}). Spectra were normalized; therefore the concentration of particular groups is proportional to the vibration band intensity. The spectra of "oligo GC centre" oligonucleotide (Fig. 6) were slightly different than the spectra of plasmid. In the spectral region between 1700 and 1400 cm^{-1}, the spectra of native plasmid DNA and "oligo GC centre" oligonucleotide samples were very similar. Remarkably, the absorption band maximum assigned to thymine varied only slightly, being 1655 cm^{-1} in native plasmid pTZ57R DNA spectra while in "oligo GC centre" oligonucleotide spectra the band was observed at 1650 cm^{-1}. Moreover, the intensity of cytosine absorption band (at 1400 cm^{-1}) was higher in the spectrum of the oligo GC centre than in plasmid spectra, indicating higher content of these groups.

FT-IR spectra of AV-153, plasmid DNA and AV-153:plasmid pTZ57R DNA at a ratio of 1:5 and incubated for 2 h are shown in

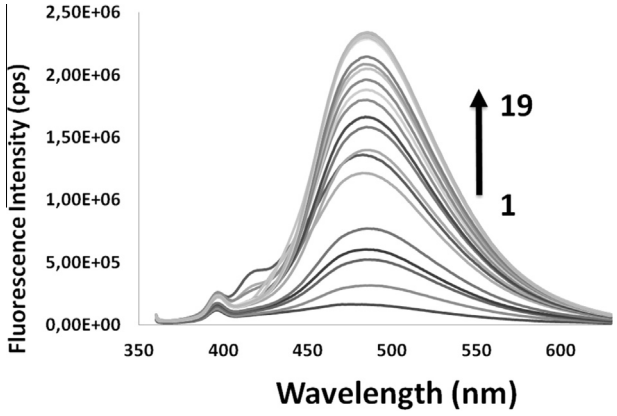

Fig. 4. AV-153 fluorescence spectra with excitation at $\lambda = 350$ nm in absence and presence of different concentrations of pTZ57R plasmid DNA. $C_{AV\text{-}153}$=25 μM, DNA concentration was increased for 12.5 μM at each step (C_{DNA}=12.5–225 μM).

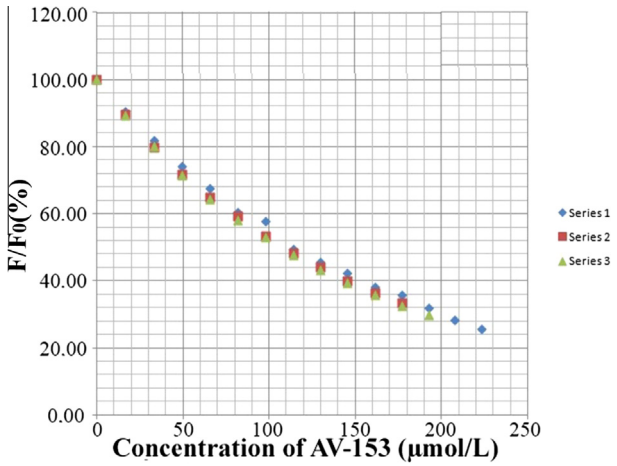

Fig. 5. Fluorescence quenching plot of the ethidium bromide-rat liver DNA complex as a function of AV-153 concentration.

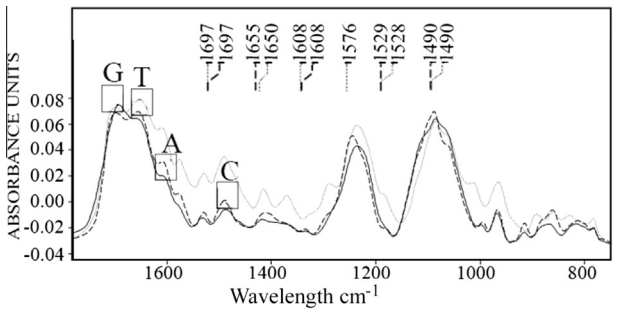

Fig. 6. FT-IR spectra of sonicated pTZ57R plasmid DNA (––––), native pTZ57R plasmid DNA (- - -) and "oligo GC center" oligonucleotide (·····). Where marked are the absorption bands assigned to guanine (G), thymine (T), adenine (A) and cytosine (C).

Fig. 7. The profile of AV-153 spectra shows many sharp bands in the region of 1000–1700 cm^{-1}. The two most intensive bands are at 1234 and 1675 cm^{-1}. In the spectra of plasmid there are three broad absorption bands with maximums at 1085, 1235 and 1680 cm^{-1} assigned to PO_2 symmetric stretching vibrations, PO_2 asymmetric stretching vibrations and CO stretching vibrations of DNA bases respectively. Moreover, the DNA bases guanine (1692 cm^{-1}), thymine (1659 cm^{-1}), adenine (1609 cm^{-1}) and

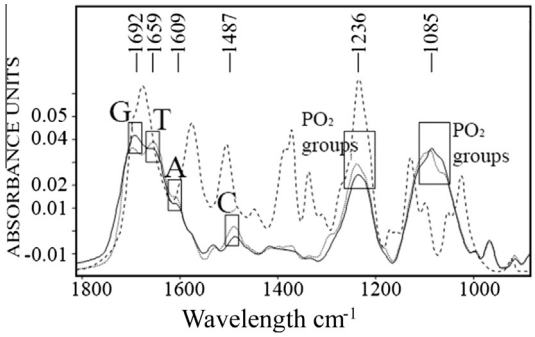

Fig. 7. FT-IR spectra of pTZ57R plasmid DNA (––––); AV-153 (- - -); pTZ57R plasmid DNA: AV-153 after 2 h of incubation (·····). Spectra are baseline-corrected and vector-normalized.

cytosine (1487 cm^{-1}) can be identified. The spectra of AV-153 and plasmid revealed wavelength shifts or intensity changes of bands characteristic for PO_2 groups and DNA bases (Fig. 7.). It has been reported [29–32] that an increase of absorption band intensities indicates partial helix destabilization of DNA but a decrease indicates stabilization of DNA, interaction with substances, and conformational changes of the biopolymer. The binding of PO_2 groups with AV-153 was indicated not only by the wavelength shift, but also the decrease in the intensity ratio of the PO_2 symmetric vibration band (with maximum at 1085 cm^{-1}) and asymmetric vibration band (with maximum at 1236 cm^{-1}) intensities. The difference spectra of AV-153 and plasmid at a ratio of 1:5 and plasmid pTZ57R spectra showed positive and negative peaks. It has been reported [29–31] that positive peaks in difference spectra and their wavelength shifts indicate the binding of DNA with a substance. The difference spectra of AV-153 with plasmid and plasmid alone showed positive peaks at 1236 cm^{-1} (PO_2 groups), 1492 cm^{-1} (cytosine), 1656 cm^{-1} (thymine) and 1708 cm^{-1} (guanine), therefore indicating the binding of both components. The second derivative spectra of AV-153, plasmid pTZ57R, and their mixture at a ratio of 1:5 were evaluated to more precisely learn which DNA bases bind with AV-153. It can be seen that the band profiles and wavelength in spectral regions characteristic of guanine, thymine and cytosine bands have changed. These data indicate binding of these DNA bases with AV-153. It should be noted that the adenine band at 1603 cm^{-1} did not shift and the peak profile was not changed, indicating a lack of binding with AV-153 (Fig. 8).

4. Discussion

In the present study, we tested the mechanisms of AV-153 interaction with DNA. Docking experiments predicted intercalation of the compound in DNA nick and in vicinity of two different

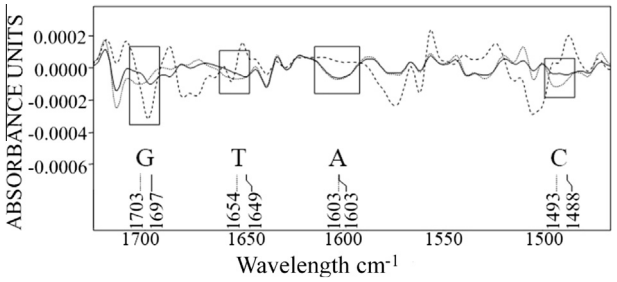

Fig. 8. The second derivative spectra of pTZ57R plasmid DNA (––––); AV-153 (- - -) and AV-153: pTZ57R plasmid DNA 1:5 after 2 h of incubation (·····). Spectra were baseline-corrected and vector-normalized.

pyrimidines. Our experiments have substantiated this model. The hyperchromic effect observed during spectrophotometric titration indicated direct binding of the molecule to DNA. The increase of intensity of fluorescence of the compound in the presence of DNA confirms this conclusion. A similar increase of fluorescence of the compound after binding to DNA was reported for 3-hydroxuflavone [33] and several steroidal pyran-based derivatives [34]. Increase is interpreted as a decrease in the fluorescence quenching effect of solvent molecules after penetration of the molecule in hydrophobic environment [34], indicating again the fact of intercalation.

The binding affinity was insensitive to DNA fragmentation by ultrasound, which produced small double-stranded fragments. Base modification by peroxynitrite, without generation of DNA strand breaks, is apparent from the lack of changes in the distribution of plasmid forms, as evaluated by electrophoresis in neutral conditions. On the contrary, the modifications manifested themselves as alkali-labile sites during electrophoresis in alkaline conditions. On the other hand, massive induction of single-strand breaks in Fenton's reaction increased affinity of the binding. Favorable binding sites between two pyrimidines were indirectly indicated by decreased affinity of the compound to AT- or GC-rich DNA. Low affinity, along with different changes in spectra of the compound when titrated by oligonucleotides lacking such structures, leads to the same conclusion. FTIR experiments provide direct evidence for preferential interactions of the compound with cytosine and thymine. Ethidium bromide competition curves clearly indicate that AV-153 intercalates in DNA.

In our opinion, the DNA repair-enhancing effect of the compound is attained via a pathway different from serving as substrate for PARP as suggested previously [19]. Intercalation of the substance in DNA can affect the level of superhelicity of the DNA molecule in the cell, thus having the capability to trigger activity of DNA repair systems [35–37] and favor PARP binding [38]. On other hand intercalation, being a DNA lesion *per se*, can activate DNA repair regulation pathways leading to increased efficiency in the repair of lesions produced by other genotoxic agents [39,40]. The exact mechanism of the antimutagenic action of the compound could be elucidated by determination of activated intracellular pathways using transcriptomic or proteomic approaches.

Conflict of Interest

The authors declare that there are no conflicts of interest.

Transparency Document

The Transparency document associated with this article can be found in the online version.

Acknowledgements

The work was supported from National Research Program 2014 "Biomedicine" and grant of the Latvian Council of Science 278/2012.

We thank U. Kalnenieks and R. Rutkis (Institute of Microbiology and Biotechnology of the University of Latvia) for giving access to their equipment. Technical assistance of K. Stebele and K. Shvirksts is highly acknowledged. We thank A.J. Sipols for editing the manuscript. Special thanks to N.P. Bazhulina (V.A. Engelhardt Institute of Molecular Biology, RAS, Moscow, Russia) for reading the manuscript and helpful comments.

References

[1] K. Magnander, K. Elmroth, Biological consequences of formation and repair of complex DNA damage, Cancer Lett. 327 (1–2) (2012) 90–96.
[2] M.P. Stone, H. Huang, K.L. Brown, G. Shanmugam, Chemistry and structural biology of DNA damage and biological consequences, Chem. Biodivers. 9 (2011) 1571–1615.
[3] V. Selvaraju, M. Joshi, S. Suresh, J.A. Sanchez, N. Maulik, G. Maulik, Diabetes, oxidative stress, molecular mechanism and cardiovascular disease – an overview, Toxicol. Mech. Methods 22 (5) (2012) 330–335.
[4] E. Tatsch, G.V. Bochi, S.J. Piva, J.A. De Carvalho, H. Kober, V.D. Torbitz, T. Duarte, C. Signor, A.C. Coelho, M.M. Duarte, G.F. Montagner, I.B. Da Cruz, R.N. Moresco, Association between DNA strand breakage and oxidative, inflammatory and endothelial biomarkers in type 2 diabetes, Mutat. Res. 732 (1–2) (2012) 16–20.
[5] A. Supriya Simon, D. Dinesh Roy, V. Jayapal, T. Vijayakumar, Somatic DNA damages in cardiovascular autonomic neuropathy, Indian J. Clin. Biochem. 1 (2011) 50–56.
[6] C. Algire, O. Moiseeva, X. Deschênes-Simard, L. Amrein, L. Petruccelli, E. Birman, B. Viollet, G. Ferbeyre, M.N. Pollak, Metformin reduces endogenous reactive oxygen species and associated DNA damage, Cancer Prev. Res. (Phila.) 5 (4) (2012) 536–543.
[7] K. Aziz, S. Nowsheen, G. Pantelias, G. Iliakis, V.G. Gorgoulis, A.G. Georgakilas, Targeting DNA damage and repair: embracing the pharmacological era for successful cancer therapy, Pharmacol. Ther. 133 (3) (2012) 334–501.
[8] K. Chong-Han, Dietary lipophilic antioxidants: implications and significance in the aging process, Crit. Rev. Food Sci. Nutr. 50 (10) (2010) 931–937.
[9] N.K. Janjua, A. Siddiqa, A. Yaqub, S. Sabahat, R. Qureshi, S. ul Haque, Spectrophotometric analysis of flavonoid-DNA binding interactions at physiological conditions, Spectrochim. Acta A Mol. Biomol. Spectrosc. 74 (2009) 1135–1137.
[10] M. Rossi, R. Meyer, P. Constantinou, F. Caruso, D. Castelbuono, M. O'Brien, V. Narasimhan, Molecular structure and activity toward DNA of baicalein, a flavone constituent of the Asian herbal medicine "Sho-saiko-to", J. Nat. Prod. 64 (1) (2001) 26–31.
[11] R. Solimani, Quercetin and DNA in solution: analysis of the dynamics of their interaction with a linear dichroism study, Int. J. Biol. Macromol. 18 (4) (1996) 287–295.
[12] R. Solimani, The flavonols quercetin, rutin and morin in DNA solution: UV–vis dichroic (and mid-infrared) analysis explain the possible association between the biopolymer and a nucleophilic vegetable-dye, Biochim. Biophys. Acta 1336 (2) (1997) 281–294.
[13] P.W. Thulstrup, T. Thormann, J. Spanget-Larsen, H.C. Bisgaard, Interaction between ellagic acid and calf thymus DNA studied with flow linear dichroism UV–VIS spectroscopy, Biochem. Biophys. Res. Commun. 265 (2) (1999) 416–421.
[14] S. Usha, I.M. Johnson, R. Malathi, Modulation of DNA intercalation by resveratrol and genistein, Mol. Cell. Biochem. 284 (1–2) (2006) 57–64.
[15] S. Zhang, X. Sun, Z. Jing, F. Qu, Spectroscopic analysis on the resveratrol-DNA binding interactions at physiological pH, Spectrochim. Acta A Mol. Biomol. Spectrosc. 1 (2011) 213–216.
[16] C.D. Kanakis, P.A. Tarantilis, M.G. Polissiou, H.A. Tajmir-Riahi, Interaction of antioxidant flavonoids with tRNA: intercalation or external binding and comparison with flavonoid-DNA adducts, DNA Cell Biol. 25 (2) (2006) 116–123.
[17] N.I. Ryabokon, R.I. Goncharova, G. Duburs, J. Rzeszowska-Wolny, A 1,4-dihydropyridine derivative reduces DNA damage and stimulates DNA repair in human cells in vitro, Mutat. Res. 587 (1–2) (2005) 52–58.
[18] N.I. Ryabokon, A. Cieślar-Pobuda, J. Rzeszowska-Wolny, Inhibition of poly(ADP-ribose) polymerase activity affects its subcellular localization and DNA strand break rejoining, Acta Biochim. Pol. 56 (2) (2009) 243–248.
[19] N.I. Ryabokon, R.I. Goncharova, G. Duburs, R. Hancock, J. Rzeszowska-Wolny, Changes in poly(ADP-ribose) level modulate the kinetics of DNA strand break rejoining, Mutat. Res. 637 (1–2) (2008) 173–181.
[20] S. Mazzini, M.C. Bellucci, R. Mondelli, Mode of binding of the cytotoxic alkaloid berberine with the double helix oligonucleotide d(AAGAATTCTT)(2), Bioorg. Med. Chem. 11 (4) (2003) 505–514.
[21] H. Baruah, U. Bierbach, Unusual intercalation of acridin-9-ylthiourea into the 5′-GA/TC DNA base step from the minor groove: implications for the covalent DNA adduct profile of a novel platinum-intercalator conjugate, Nucleic Acids Res. 31 (14) (2003) 4138–4146.
[22] J. Jähnchen, M.G. Purwanto, K. Weisz, NMR studies on self-complementary oligonucleotides conjugated with methylene blue, Biopolymers 79 (6) (2005) 335–343.
[23] K.M. Robinson, J.S. Beckman, Synthesis of peroxynitrite from nitrite and hydrogen peroxide, Methods Enzymol. 396 (2005) 207–214.
[24] H.R. Drew, R.M. Wing, T. Takano, C. Broka, S. Tanaka, K. Itakura, R.E. Dickerson, Structure of a B-DNA dodecamer: conformation and dynamics, Proc. Natl. Acad. Sci. U.S.A. 78 (4) (1981) 2179–2183.
[25] D.J. Diller, K.M. Merz Jr., High throughput docking for library design and library prioritization, Proteins 43 (2) (2001) 113–124.
[26] B.R. Brooks, R.E. Bruccoleri, B.D. Olafson, D.J. States, S. Swaminathan, M. Karplus, CHARMM: a program for macromolecular energy, minimization, and dynamics calculations, J. Comput. Chem. 4 (1983) 187–217.
[27] L.R. Hill, An index to deoxyribonucleic acid base compositions of bacterial species, J. Gen. Microbiol. 44 (3) (1966) 419–437.

[28] R. Ghosh, S. Bhowmik, A. Bagchi, D. Das, S. Ghosh, Chemotherapeutic potential of 9-phenyl acridine: biophysical studies on its binding to DNA, Eur. Biophys. J. 39 (8) (2010) 1243–1249.
[29] S. Nafisi, F. Manouchehri, H.-A. Tajmir-Riahi, M. Varavipour, Structural features of DNA interaction with caffeine and theophylline, J. Mol. Struct. 875 (2008) 392–399.
[30] S. Nafisi, M. Montazeri, F. Manouchehri, The effect of Se salts on DNA structure, J. Photochem. Photobiol. 113 (2012) 36–41.
[31] S.T. Saito, G. Silva, C. Pungartnik, M. Brendel, Study of DNA–emodin interaction by FTIR and UV–vis spectroscopy, J. Photochem. Photobiol. 111 (2012) 59–63.
[32] K.D. Jangir, G. Tyagi, R. Mehrotra, S. Kundu, Carboplatin interaction with calf-thymus DNA: a FTIR spectroscopic approach, J. Mol. Struct. 969 (2010) 126–129.
[33] B. Jana, S. Senapati, D. Ghosh, D. Bose, N. Chattopadhyay, Spectroscopic exploration of mode of binding of ctDNA with 3-hydroxyflavone: a contrast to the mode of binding with flavonoids having additional hydroxyl groups, J. Phys. Chem. B 116 (1) (2012) 639–645.
[34] Shamsuzzaman, A.M. Dar, Y. Khan, A. Sohail, Synthesis and biological studies of steroidal pyran based derivatives, J. Photochem. Photobiol. B 129 (2013) 36–47.
[35] M. Sun, T. Nishino, J.F. Marko, The SMC1-SMC3 cohesin heterodimer structures DNA through supercoiling-dependent loop formation, Nucleic Acids Res. 41 (12) (2013) 6149–6160.
[36] L. Hubert Jr, Y. Lin, V. Dion, J.H. Wilson, Topoisomerase 1 and single-strand break repair modulate transcription-induced CAG repeat contraction in human cells, Mol. Cell. Biol. 31 (15) (2011) 3105–3112.
[37] D. Weinstein-Fischer, M. Elgrably-Weiss, S. Altuvia, *Escherichia coli* response to hydrogen peroxide: a role for DNA supercoiling, topoisomerase I and Fis, Mol. Microbiol. 35 (6) (2000) 1413–1420.
[38] S. Chasovskikh, A. Dimtchev, M. Smulson, A. Dritschilo, DNA transitions induced by binding of PARP-1 to cruciform structures in supercoiled plasmids, Cytometry A 68 (1) (2005) 21–27.
[39] J.A. Daniel, A. Nussenzweig, The AID-induced DNA damage response in chromatin, Mol. Cell 50 (3) (2013) 309–321.
[40] M. Christmann, B. Kaina, Transcriptional regulation of human DNA repair genes following genotoxic stress: trigger mechanisms, inducible responses and genotoxic adaptation, Nucleic Acids Res. 41 (18) (2013) 8403–8420.